



Tandospirone augments cisplatin treatment by lowering cholesterol and managing distress in NSCLC patients



Xichun Qin^{1,5}, Bo Cheng^{2,5}, Shangshang Ma^{1,5}, Kun Li^{1,5}, Yongfei Fan¹, Mingjun Li¹, Rangrang Wang¹, Xuefeng Ai¹, Leilei Wu³✉, Xiucheng Liu¹✉, Xiaojin Wu⁴✉ & Dong Xie¹✉

Emotional distress (ED), including anxiety and depression, is highly prevalent in patients with non-small cell lung cancer (NSCLC) and may compromise both quality of life and treatment outcomes. In this study, we evaluated the mental health status of 1185 surgically treated NSCLC patients and developed a predictive model integrating clinical and demographic factors. Adjuvant therapy after lung cancer surgery was associated with an increased risk of ED, particularly chemotherapy. To address safety concerns, we further examined commonly used anti-ED drugs in experimental models and found no evidence of tumor-promoting effects. Importantly, tandospirone not only alleviates ED but also enhances the therapeutic efficacy of cisplatin. These findings highlight the clinical importance of systematic ED management in lung cancer care and suggest tandospirone as a promising candidate that may simultaneously support psychological well-being and improve chemotherapy response, offering a more comprehensive treatment strategy for NSCLC patients.

Lung cancer remains one of the most prevalent and deadly malignancies worldwide, posing a severe threat to public health^{1,2}. Despite substantial advancements in diagnosis and treatment, surgical resection remains the primary therapeutic approach for early-stage non-small cell lung cancer (NSCLC)³. However, postoperative patients often experience a range of physical and psychological challenges⁴. Emotional distress (ED), commonly manifesting as depression and/or anxiety, is a frequent psychological complication following lung cancer surgery. The incidence of ED in lung cancer patients is significantly higher than that in the general population, adversely affecting their quality of life and potentially influencing treatment outcomes and prognosis^{5,6}. Therefore, identifying effective interventions for ED in postoperative lung cancer patients is of great clinical significance.

The underlying mechanisms of ED are complex and involve physiological, psychological, and social factors. Postoperative pain, physical limitations, fear of disease recurrence, and uncertainty about the future all contribute to ED^{7,8}. Furthermore, many early-stage lung cancer patients undergo adjuvant therapies such as chemotherapy, immunotherapy, and targeted therapy post-surgery, which may exacerbate ED symptoms^{9–11}. However, research on the interaction between anti-ED medications and lung cancer treatment remains limited. Clinically, anti-ED drugs are widely

prescribed for various anxiety and depression disorders. However, for postoperative lung cancer patients, especially those receiving adjuvant therapy, their safety profile and potential impact on tumor growth remain critical concerns. While some epidemiological studies have suggested that anti-ED drugs may influence tumor progression through direct effects on cancer cells or by modulating neurotransmitter levels and the immune microenvironment^{12–14}, their specific mechanisms and clinical implications remain unclear. Therefore, effective ED management in postoperative lung cancer patients requires not only psychological interventions but also a thorough evaluation of pharmacological treatments' feasibility and safety.

Given this context, we conducted a large-scale clinical survey involving 1185 patients undergoing lung cancer surgery. Our goal was to systematically evaluate postoperative mental health and examine the correlation between ED and adjuvant therapies. Our findings revealed a significantly higher incidence of anxiety and depression in patients receiving chemotherapy than in other treatment groups, indicating that chemotherapy may be a major risk factor for ED. To explore potential pharmacological interventions, we systematically evaluated the effects of commonly used anti-anxiety and anti-depressant drugs in combination with cisplatin chemotherapy in both cell and animal models. Among these, tandospirone

¹Department of Thoracic Surgery, Shanghai Pulmonary Hospital, School of Medicine, Tongji University, Shanghai, 200433, China. ²Department of Neurology, Tongji Hospital, School of Medicine, Tongji University, 389 Xincun Road, Shanghai, 200292, China. ³Department of Thoracic Surgery, Hangzhou Institute of Medicine (HIM), Zhejiang Cancer Hospital, Chinese Academy of Sciences, Hangzhou, 310005, China. ⁴Department of Radiation Oncology, Xuzhou Central Hospital, Xuzhou Clinical School of Xuzhou Medical University, Jiefang South Road, No. 199, Xuzhou, 221000, China. ⁵These authors contributed equally: Xichun Qin, Bo Cheng, Shangshang Ma, Kun Li. ✉e-mail: wull@zjcc.org.cn; lxch2020@163.com; wuxiaojinxz@126.com; xiedong@tongji.edu.cn

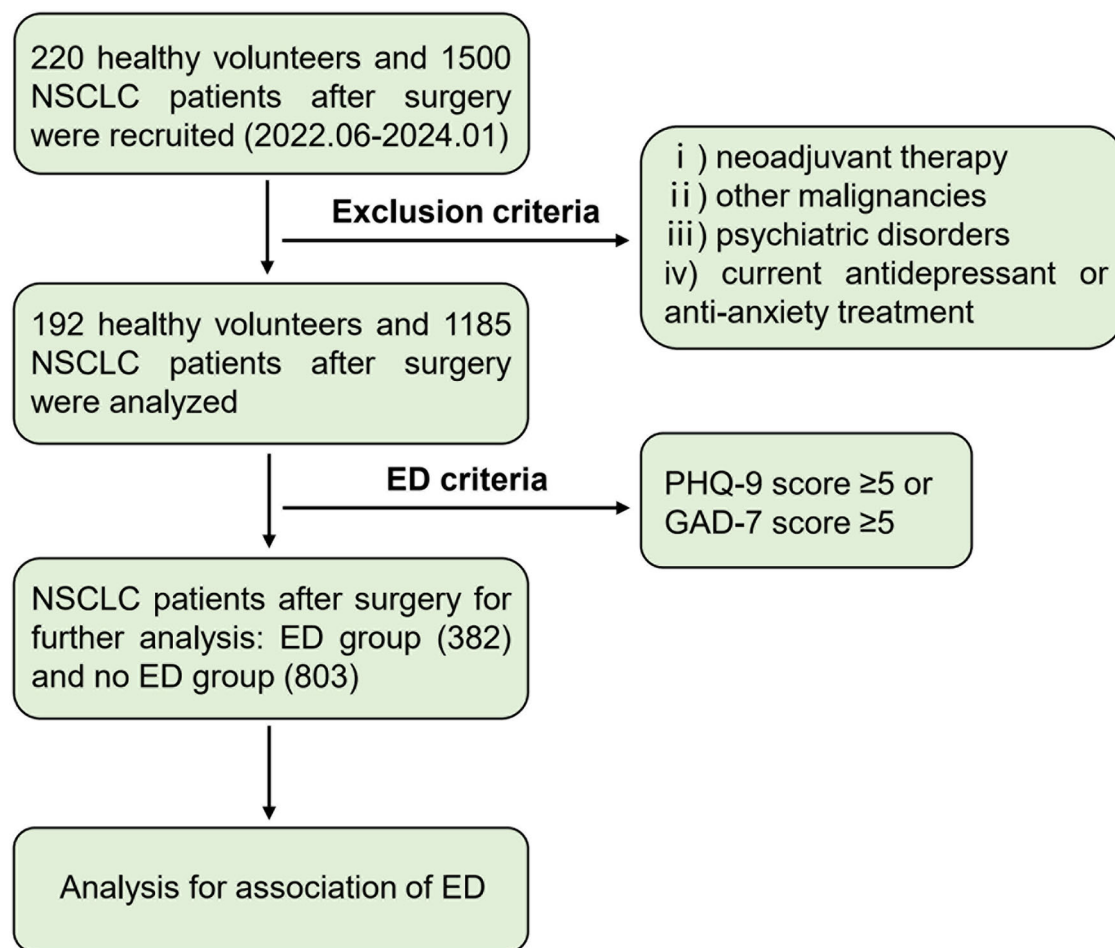


Fig. 1 | Flow chart of the selected population in this study.

lowers cholesterol levels in tumor cells, thereby enhancing their susceptibility to apoptosis. These findings suggest that tandospirone may serve a dual function: alleviating ED symptoms and enhancing chemotherapy efficacy, providing a novel avenue for integrative lung cancer treatment strategies.

Results

NSCLC patients have a significantly increased risk of ED after surgery

A total of 1500 NSCLC patients who underwent surgical resection and 220 healthy volunteers were recruited from our center for a comprehensive questionnaire-based assessment. Patients with incomplete data, a history of neoadjuvant therapy, other malignancies within the past 3 years, pre-existing psychiatric disorders, or those currently receiving antidepressant or anti-anxiety treatment were excluded from the study. The final analysis included 1185 NSCLC patients and 192 healthy controls (Fig. 1). Demographic characteristics were similar between the healthy population and postoperative patients (Table 1). However, the prevalence of ED among healthy individuals was only 8.9%, whereas it was significantly higher in postoperative NSCLC patients, reaching 32.2% ($P < 0.001$). These findings underscore a markedly increased risk of ED following lung cancer surgery.

Chemotherapy is an independent risk factor for increased ED in NSCLC patients after surgery

To identify key risk factors associated with ED, we stratified postoperative NSCLC patients into ED and non-ED groups. Compared with the non-ED group, patients in the ED group were older, had a higher proportion of females, a greater prevalence of diabetes, a significantly higher prevalence of

hypertension, a lower education level, and a higher rate of lymph node metastasis ($P < 0.05$). No statistically significant differences were observed in smoking history or tumor T stage (Table 2). According to the type of postoperative adjuvant therapy, 602 patients received no treatment, 80 patients received chemotherapy, 246 patients received chemotherapy combined with other treatments (such as targeted therapy or immunotherapy), and 253 patients received other treatments without chemotherapy (Fig. 2A). Further analysis of treatment modalities revealed a significant association between chemotherapy and increased ED incidence (Fig. 2B and Supplement Table 2).

To predict the risk of postoperative anxiety and depression in patients with lung cancer, two supervised machine learning algorithms were applied. In the test set, the Random Forest (RF) model achieved an AUC of 0.91 (Fig. 2C), outperforming the Support Vector Machine (SVM) model (Supplement Fig. 1), which yielded an AUC of 0.66. Model interpretation indicated that postoperative treatment was the most influential factor associated with the occurrence of emotional disorders after surgery (Fig. 2D). Multivariate regression analysis confirmed chemotherapy as an independent risk factor for ED (Supplement Table 3 and Supplement Table 4). These findings suggest that patients undergoing chemotherapy after NSCLC surgery face an elevated risk of psychological distress.

Common anti-ED drugs do not promote tumor cell progression and may enhance chemotherapy effects in patients with ED

We systematically evaluated the impact of six commonly prescribed anti-ED drugs on lung cancer cell proliferation and apoptosis. The selected medications included paroxetine and sertraline in selective serotonin reuptake inhibitors (SSRIs); bupropion in norepinephrine-dopamine

Table 1 | Demographics and characteristics of patient

Variables	Total (n = 1377)	Healthy (n = 192)	Surgery (n = 1185)	P-value
Age, years (%)				0.908
<65	1196 (86.9)	168 (87.5)	1028 (86.8)	
≥65	181 (13.1)	24 (12.5)	157 (13.2)	
Sex (male/female)	551/826	78/114	473/712	0.874
Smoking history (%)	369 (26.8)	49 (25.5)	320 (27.0)	0.726
Drinking history (%)	233 (16.9)	33 (17.2)	200 (16.9)	0.917
Hypertension (%)	362 (26.3)	48 (25.0)	314 (26.5)	0.724
Diabetes (%)	106 (7.7)	13 (6.8)	93 (7.8)	0.770
BMI				0.534
<24	731 (53.1)	106 (55.2)	625 (52.7)	
≥24	646 (46.9)	86 (44.8)	560 (47.3)	
Educational level (%)				0.148
<High school	1041 (75.6)	137 (71.4)	904 (76.3)	
≥High school	336 (24.4)	55 (28.6)	281 (23.7)	
Emotional distress (%)	399 (29.0)	17 (8.9)	382 (32.2)	<0.001*

*Statistically significant values.

Table 2 | Demographics and characteristics of ED in NSCLC patients

Variables	Total (n = 1185)	ED (n = 382)	No ED (n = 803)	P-value
Age, years (%)				0.009*
<65	1028 (86.8)	316 (82.7)	712 (88.7)	
≥65	157 (13.2)	66 (17.3)	91 (11.3)	
Sex (male/female)	473/712	131/251	342/461	0.006*
Smoking history (%)	320 (27.0)	93 (24.3)	227 (28.3)	0.162
Drinking history (%)	200 (16.9)	58 (15.2)	142 (17.7)	0.319
Hypertension (%)	314 (26.5)	122 (31.9)	192 (23.9)	0.004*
Diabetes (%)	93 (7.8)	41 (10.7)	52 (6.5)	0.001*
BMI				0.319
<24	625 (52.7)	193 (50.5)	432 (53.8)	
≥24	560 (47.3)	189 (49.5)	371 (46.2)	
Educational level (%)				0.002*
<High school	904 (76.3)	313 (81.9)	591 (73.6)	
≥High school	281 (23.7)	69 (18.1)	212 (26.4)	
Tumor stage (%)				0.232
I	946 (79.8)	294 (77.0)	652 (81.2)	
II	221 (18.7)	81 (21.2)	140 (17.4)	
III	18 (1.5)	7 (1.8)	11 (1.4)	
IV	0	0	0	
Lymph node metastasis (%)				0.024*
Negative	902 (76.1)	275 (72.0)	627 (78.1)	
Positive	283 (23.9)	107 (28.0)	176 (21.9)	
Distant metastasis (%)				N/A
M0	1185 (100.0)	382 (100.0)	803 (100.0)	
M1	0	0	0	

*Statistically significant values.

reuptake inhibitor (NDRIs); amitriptyline in tricyclic antidepressants (TcAs); and other drugs such as tandospirone and agomelatine (Fig. 3A). First, we conducted CCK-8 assays to assess the effects of these drugs on the proliferation of two NSCLC cell lines (A549 and H1299) across a concentration range of 0–200 µg/mL. None of the six medications significantly

promoted tumor cell proliferation. Instead, all displayed a mild inhibitory effect on cell growth at higher concentrations (Fig. 3B, C). This result suggests that these anti-ED drugs slightly inhibit lung cancer cell progression within the commonly used clinical dose range. To further explore their influence on tumor cell survival, we standardized the drug concentration to

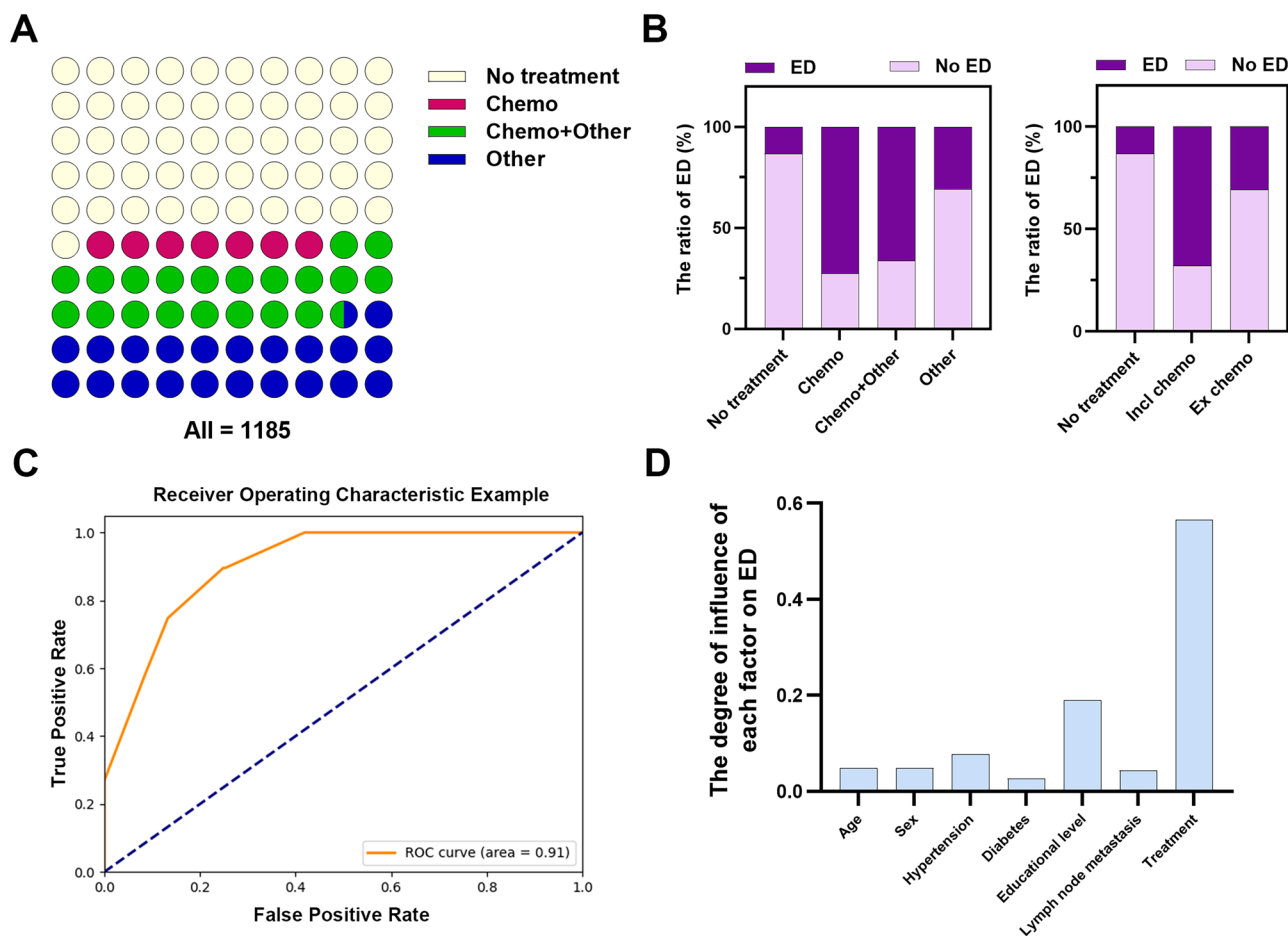


Fig. 2 | Patients receiving chemotherapy have a significantly increased risk of ED. **A** Waffle chart of statistics on postoperative adjuvant therapy for NSCLC patients. **B** Statistics of ED patients and non-ED patients according to postoperative adjuvant treatment methods. Inclusive chemotherapy: Any adjuvant treatment including chemotherapy; Excluding chemotherapy: Any adjuvant treatment that does not

include chemotherapy. **C** ROC curve of the Random Forest model for predicting postoperative ED in patients with lung cancer. **D** Bar plot showing the relative importance of key predictors for postoperative ED based on the final Random Forest model. Postoperative treatment was identified as the most influential factor.

100 µg/mL and performed flow cytometry analysis to assess apoptosis induction (Fig. 3D, E). All six drugs induced some degree of apoptosis in A549 and H1299 cells, with tandospirone and sertraline exhibiting the most pronounced effects (apoptosis rates of 7.2% and 9.9%, respectively).

We then examined the interactions between these anti-ED drugs and cisplatin chemotherapy. None of the medications reduced the sensitivity of A549 or H1299 cells to cisplatin; rather, they increased chemotherapy efficacy to varying degrees (Fig. 3F, G). This suggests that these anti-ED drugs do not reduce the chemotherapeutic effectiveness of cisplatin. Notably, tandospirone exhibited a significant synergistic effect, markedly increasing cisplatin-induced cytotoxicity in both cell lines. These results indicate that tandospirone may have an unexpected function of enhancing chemotherapy.

Tandospirone enhances the anti-tumor effects of cisplatin

Tandospirone is a non-benzodiazepine anxiolytic that alleviates anxiety and depressive symptoms by modulating the serotonin (5-HT) system¹⁵. It is widely used for the long-term treatment of generalized anxiety disorder and depression¹⁶. However, its role in tumor biology remains unexplored. To investigate the therapeutic potential of tandospirone in augmenting cisplatin’s antitumor effects, we conducted a comprehensive evaluation using both in vitro and in vivo models. The cloning sphere experiment revealed that NSCLC cells treated with the tandospirone-cisplatin combination exhibited significantly reduced clonogenic capacity compared with the

cisplatin monotherapy group. The number and size of tumor cell colonies were significantly diminished, suggesting that the combination therapy effectively impairs the self-renewal ability of cancer stem-like cells (Fig. 4A). Furthermore, flow cytometry analysis demonstrated that the cell apoptosis rate was significantly higher in cells treated with the tandospirone-cisplatin combination than in those treated with cisplatin alone (Fig. 4B). These results indicate that tandospirone enhances cisplatin-induced apoptosis, thereby increasing tumor cell susceptibility to chemotherapy. To further assess its impact on tumor progression, we conducted Transwell invasion and scratch wound-healing assays. The combination treatment significantly suppressed tumor cell migration and invasion, as evidenced by a substantial reduction in both the number of transmembrane invasive cells and wound closure rates (Fig. 4C, D). These findings suggest that tandospirone exerts a synergistic effect in limiting tumor cell dissemination.

To validate these findings in an animal model, we established a subcutaneous xenograft model and a lung metastasis model using A549 cells injected via the tail vein of nude mice (Fig. 4E). In the subcutaneous tumor model, mice receiving the tandospirone-cisplatin combination exhibited significantly slower tumor growth compared with those treated with cisplatin alone. Final tumor weight was also significantly lower in the combination therapy group than in the cisplatin monotherapy group, indicating that tandospirone enhances the inhibitory effect of cisplatin (Fig. 4F–H and Supplementary Fig. 2). The lung metastasis model further corroborated these results, showing a marked reduction in

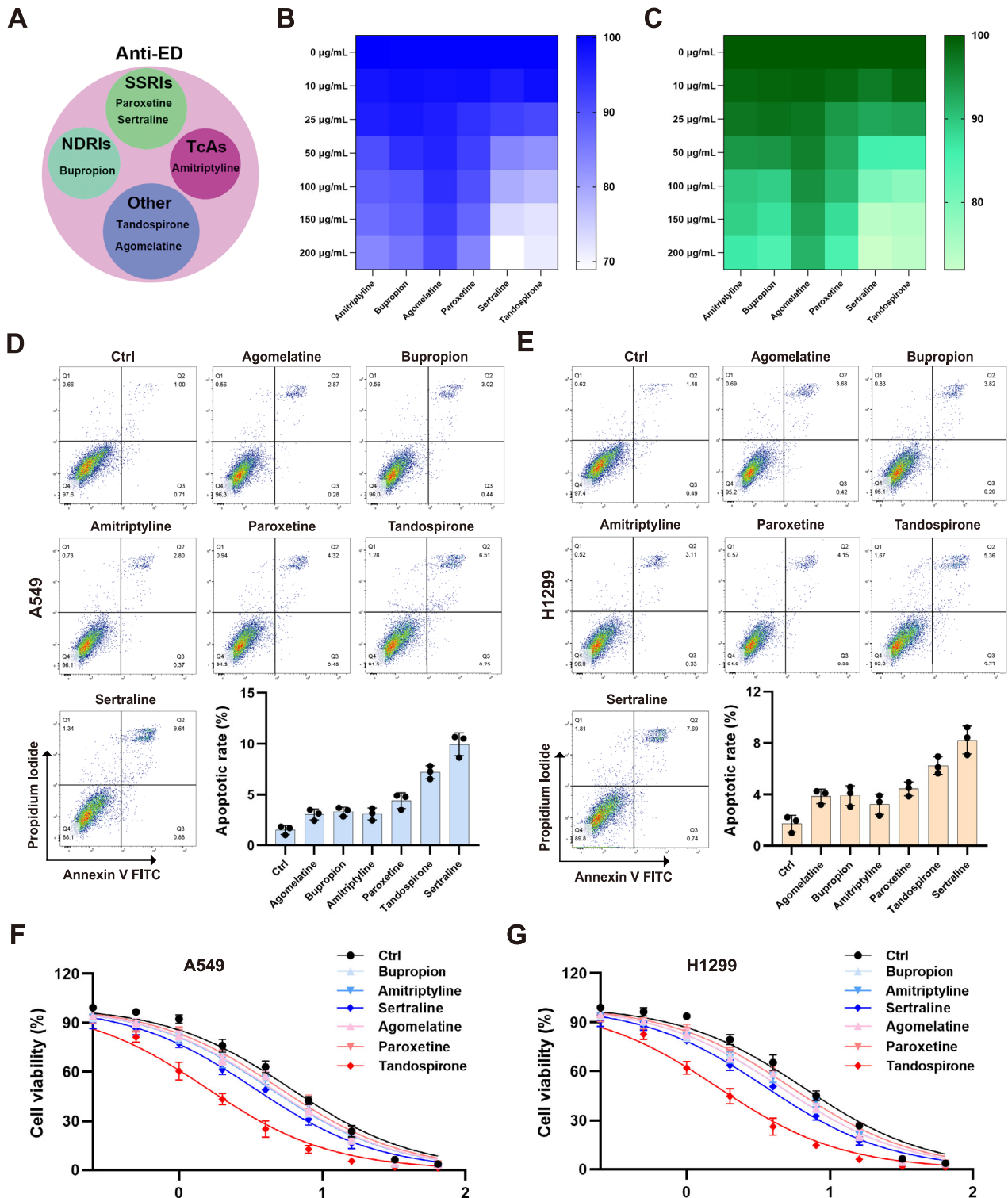


Fig. 3 | Drugs commonly used by ED patients do not promote tumor growth or affect chemotherapy. A Anti-ED drugs include SSRIs (paroxetine, sertraline), NDRIs (bupropion), TcAs (amitriptyline), and others such as tandospirone and agomelatine. Heat map display of cell viabilities of A549 (B) and H1299 (C) cells after incubation with different concentrations of anti-ED drugs for 48 h. Effects of

various anti-ED drugs (100 µg/mL) on apoptosis of A549 (D) and H1299 (E) cells after 48 h of incubation. Effects of various anti-ED drugs (100 µg/mL) combined with different concentrations of cisplatin (DDP) on the viability of A549 (F) and H1299 (G) cells. The x-axis values are expressed as $\log_{10}([DDP], \mu M)$.

metastatic nodules in the combination treatment group compared with the cisplatin monotherapy group, suggesting that tandospirone not only inhibits primary tumor growth but also plays a crucial role in preventing distant metastases (Fig. 4I, J). To assess the impact of combined therapy

on tumor cell proliferation, we performed Ki67 IHC staining and quantitative analysis on mouse tumor tissues. Quantitative analysis revealed a significant decrease in Ki67-positive cells in the combination treatment group compared with the cisplatin monotherapy group. This

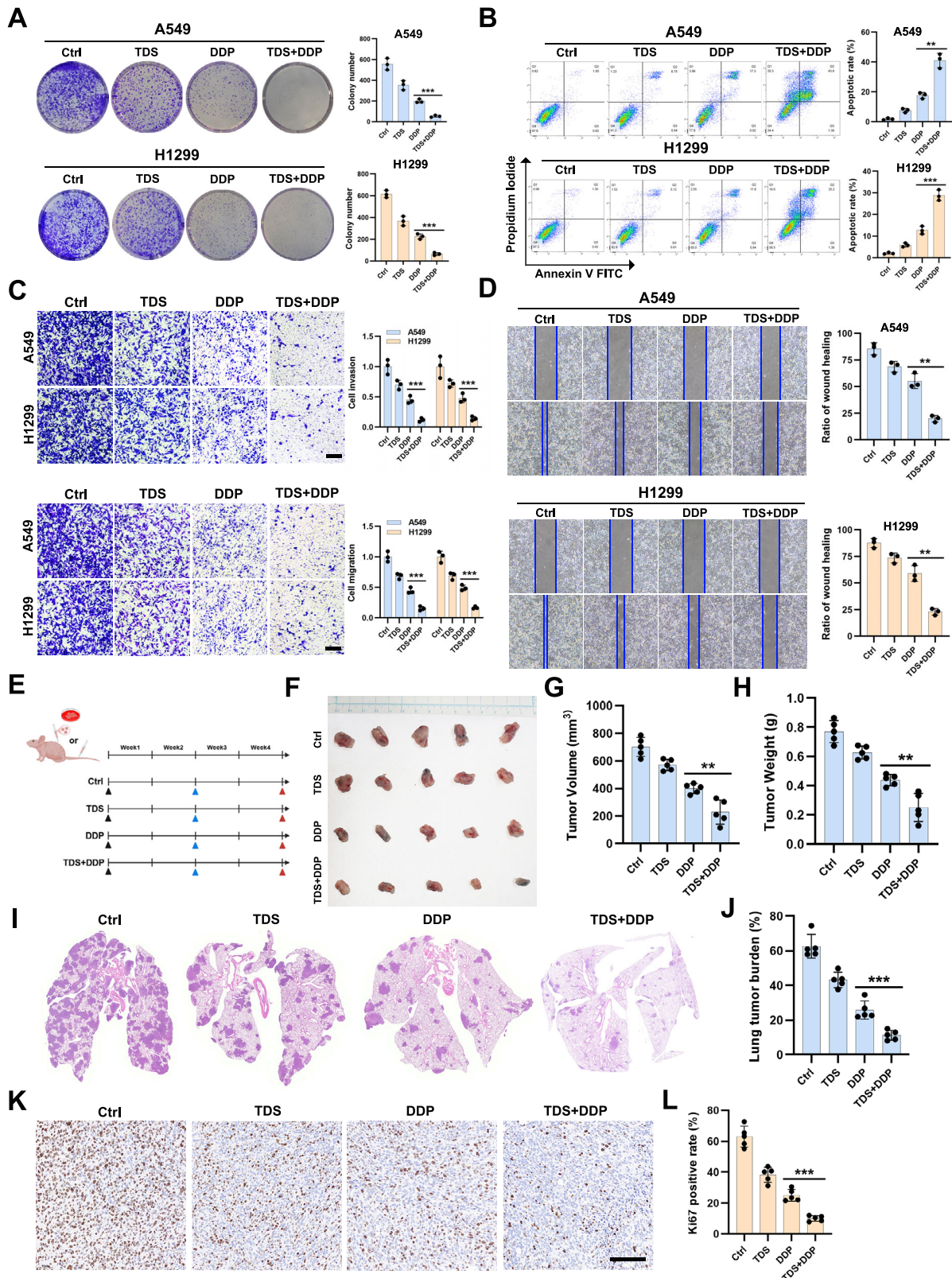


Fig. 4 | Tansospirone enhances the anti-tumor effect of cisplatin. **A** Colony formation assay was performed to determine the effect of tansospirone (100 µg/mL) on the proliferation of cisplatin (DDP)-treated A549 and H1299 cells. Quantitative analysis is presented on the right ($n = 3$). **B** Flow cytometry was performed to determine the effect of tansospirone on the apoptosis of DDP-treated A549 and H1299 cells. Quantitative analysis is presented on the right ($n = 3$). **C** Migration and invasion of A549 and H1299 cells treated with tansospirone combined with DDP. Quantitative analysis is presented on the right ($n = 3$), Scale bar = 100 µm. **D** The wound healing assay revealed that tansospirone enhances DDP-induced inhibition

of A549 and H1299 cell migration. Quantitative analysis is presented on the right ($n = 3$). **E** Schematic diagram of in vitro experimental model. Drug treatments were initiated 2 weeks after tumor establishment. **F–H** The effects of tansospirone combined with cisplatin on tumor size, weight, and volume are assessed using the mouse xenograft model ($n = 5$). **I, J** HE staining and quantitative analysis of lung metastatic nodules in xenograft tumors. **K, L** IHC staining and Ki67 quantification in xenograft tumors, Scale bar = 200 µm. Data are expressed as the mean \pm SD, $**P < 0.01$, $***P < 0.001$.

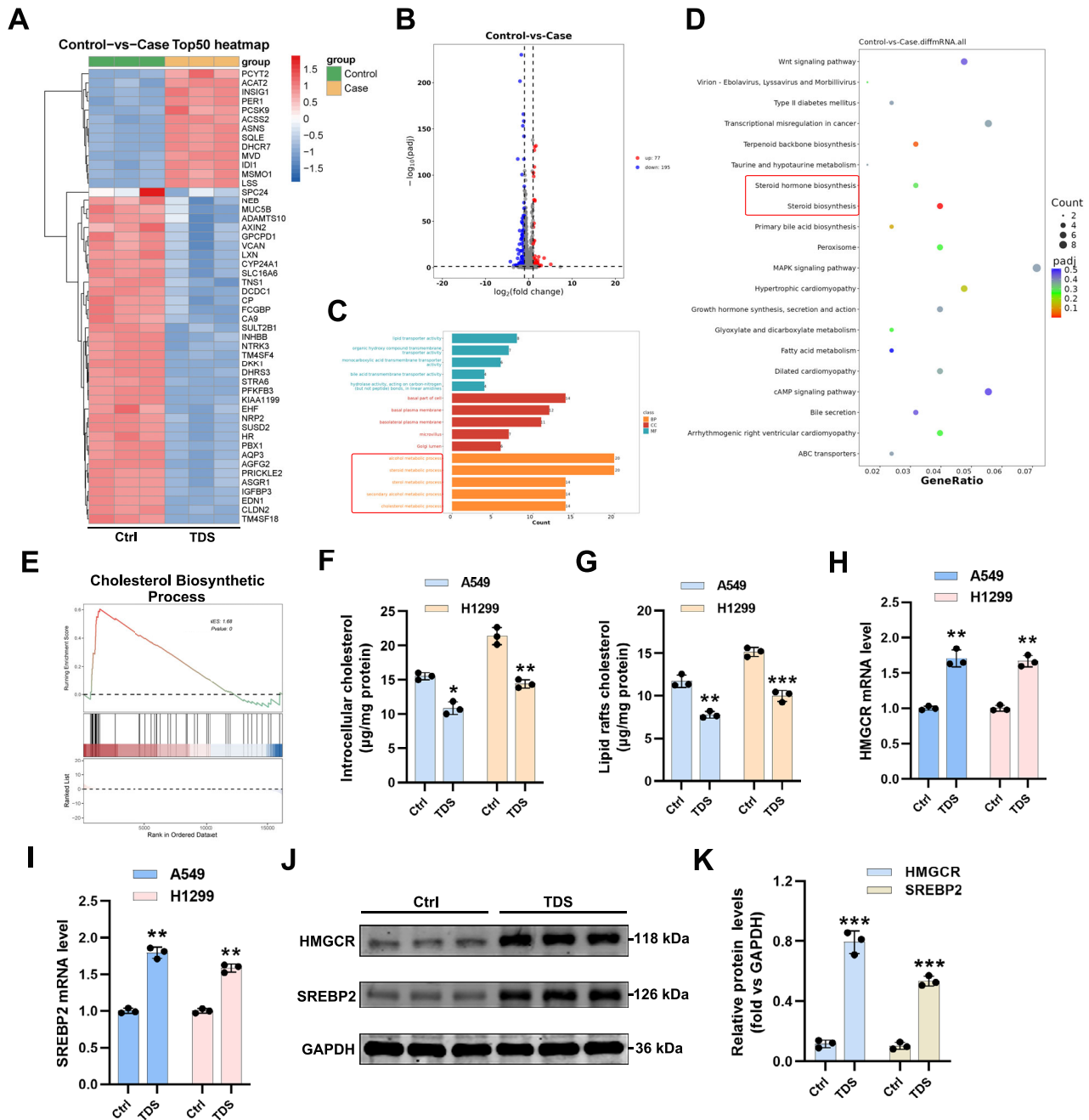


Fig. 5 | Tandospirone decreases the cholesterol levels in tumor cells. **A** Heat map display of the top 50 genes of A549 cells after tandospirone (100 $\mu\text{g}/\text{mL}$) treatment. **B** Volcano plot depicting differentially expressed genes ($|\text{fold change}| \geq 1.0$, $padj < 0.05$) in the TDS group vs. Ctrl group. **C**, **D** GO and KEGG pathway enrichment analysis was conducted on differentially expressed genes. **E** GSEA of TDS and Ctrl groups by using a cholesterol biosynthetic process signature. **F**, **G** The

cholesterol level in the cytoplasm or lipid rafts of A549 and H1299 cells. **H**, **I** The levels of HMGCR and SREBP2 were determined by qRT-PCR analysis of A549 and H1299 cells. **J**, **K** Western blotting revealed that the levels of HMGCR and SREBP2 are increased in A549 cells treated with TDS. Data are expressed as the mean \pm SD, $n = 3$, $*P < 0.05$, $**P < 0.01$, $***P < 0.001$.

reduction in proliferative activity provides further evidence of the enhanced anti-tumor efficacy of tandospirone in combination with cisplatin (Fig. 4K, I).

Tandospirone reduces cholesterol levels in tumor cells

To elucidate the molecular mechanism by which tandospirone enhances cisplatin sensitivity, we conducted RNA-seq transcriptomic analysis on A549 cells treated with tandospirone. The analysis identified 272 differentially expressed genes (screening condition: $|\text{fold change}| \geq 1.0$, $Padj < 0.05$) (Fig. 5A, B). Gene Ontology (GO) functional enrichment and

Kyoto Encyclopedia of Genes and Genomes (KEGG) pathway enrichment analyses revealed a significant enrichment of cholesterol synthesis-related pathways (Fig. 5C, D and Supplementary Fig. 3A). Additionally, Gene Set Enrichment Analysis further confirmed that cholesterol biosynthesis pathways and steroid biosynthesis were markedly altered in response to tandospirone treatment (Fig. 5E and Supplementary Fig. 3B). These findings suggest that tandospirone may exert its chemotherapysensitizing effects by modulating cholesterol metabolism.

To validate this hypothesis, we measured intracellular cholesterol levels in A549 and H1299 cells following tandospirone treatment. Compared with

untreated controls, tansospirone significantly reduced both total intracellular cholesterol and membrane-associated cholesterol (Fig. 5F, G). This indicates that tansospirone effectively disrupts cholesterol homeostasis in tumor cells. To further explore the regulatory mechanisms underlying this cholesterol depletion, we examined key genes involved in cholesterol biosynthesis. qPCR and western blot analyses (Fig. 5H–K and Supplementary Fig. 4A, B) demonstrated that tansospirone treatment led to a significant upregulation of 3-hydroxy-3-methylglutaryl-CoA reductase (HMGCR), the rate-limiting enzyme in cholesterol synthesis¹⁷, and sterol regulatory element binding protein 2 (SREBP2), a key upstream transcription factor regulating cholesterol metabolism¹⁸. This suggests that tumor cells may have initiated a feedback regulation mechanism because of the reduced cholesterol levels. Tansospirone may consume cholesterol in tumor cells and induce abnormal activation of the cholesterol synthesis pathway, thereby modifying the cell metabolic state, affecting the cell's survival and proliferation, and improving cisplatin's antitumor effect.

Reducing cholesterol levels in NSCLC cells can increase their sensitivity to apoptosis

Building on our experimental results, we speculate that reducing cholesterol levels may render tumor cells more susceptible to chemotherapy. To validate this hypothesis, we conducted additional experiments to assess the role of cholesterol depletion in tansospirone-induced cisplatin sensitization. We first supplemented A549 and H1299 cells with exogenous cholesterol to determine whether restoring cholesterol levels would counteract the sensitizing effect of tansospirone (Fig. 6B). Although exogenous cholesterol marginally promoted tumor cell proliferation (Fig. 6A), it significantly attenuated the enhanced cytotoxicity of cisplatin observed in the presence of tansospirone (Fig. 6B).

To further investigate whether cholesterol depletion alone could enhance cisplatin's antitumor effects, we treated A549 and H1299 cells with methyl- β -cyclodextrin (M β CD), a cholesterol scavenger¹⁹. Our results revealed that cholesterol depletion significantly increased cell death, indicating that reduced cholesterol levels independently contribute to enhanced chemotherapy sensitivity (Fig. 6C, D). This finding was reinforced by clonogenic assays, where M β CD-treated cells exhibited a significantly reduced capacity for colony formation, an effect that was further amplified when combined with cisplatin (Fig. 6E). Flow cytometry analysis confirmed these observations, showing a substantial increase in apoptosis in cholesterol-depleted cells, with an even more pronounced effect when co-administered with cisplatin (Fig. 6F). Furthermore, Transwell invasion and scratch assays demonstrated that cholesterol depletion also inhibited tumor cell migration and invasion. Specifically, M β CD treatment significantly reduced the number of cells crossing the membrane and slowed wound healing, with these effects being further intensified when combined with cisplatin (Supplementary Fig. 5A, B). These findings suggest that cholesterol depletion not only enhances cisplatin-induced apoptosis but also impairs tumor cell motility and metastatic potential.

To explore whether cholesterol depletion broadly sensitizes tumor cells to other forms of cell death, we tested its effects in combination with various chemotherapeutic drugs and targeted inhibitors, including cisplatin, pemetrexed, docetaxel, bortezomib (a proteasome inhibitor)²⁰, and ML162 (a GPX4 inhibitor)²¹. Remarkably, M β CD treatment significantly enhanced the cytotoxicity of all tested agents, as evidenced by a pronounced decrease in cell viability (Fig. 6G). Likewise, tansospirone also exhibited a strong synergistic effect when combined with these apoptosis-inducing agents, reinforcing the notion that cholesterol depletion serves as a metabolic vulnerability that can be exploited to enhance cancer therapy.

Discussion

In this study, we conducted a comprehensive analysis of ED in postoperative lung cancer patients, investigating its prevalence, risk factors, and potential therapeutic interventions. Additionally, we explored the impact of anti-ED drugs on tumor biology and chemotherapy sensitivity, yielding significant findings at multiple levels (Fig. 6H). Our results not only provide a scientific

foundation for clinical psychological interventions but also introduce a new approach to tumor metabolic regulation that warrants further investigation.

Lung cancer remains one of the most aggressive malignancies worldwide, with high morbidity and mortality rates^{2,22}. Despite advances in treatment, surgical resection remains the primary curative option for early- and mid-stage lung cancer patients. However, postoperative recovery extends beyond physical healing; patients frequently experience the adverse side effects of chemotherapy, fear of disease recurrence, and a decline in overall quality of life, all of which contribute to a high incidence of ED^{5,23}. Our findings indicate that ED significantly increases following lung cancer surgery and is strongly associated with adjuvant treatment, identifying chemotherapy as an independent risk factor. While anti-ED medications are commonly prescribed for patients experiencing anxiety and depression concerns persist regarding their potential interference with chemotherapy efficacy. To address this issue, we systematically screened 6 widely used anti-ED drugs, assessing their effects on cell proliferation, invasion, and migration in A549 and H1299 lung cancer cell lines. Contrary to common concerns, our results demonstrated that these drugs did not promote tumor progression. Instead, certain anti-ED medications, particularly tansospirone, exhibited unexpected tumor-suppressive effects. Notably, tansospirone not only failed to diminish the cytotoxicity of cisplatin but significantly reduced its IC₅₀, indicating a pronounced chemosensitizing effect. Tansospirone, a well-established anxiolytic that functions as a partial agonist of 5-HT_{1A} receptors¹⁸, has not been previously studied for its impact on tumor metabolism.

Through RNA-seq analysis, we identified that tansospirone induces significant alterations in cholesterol metabolism, particularly by activating cholesterol synthesis pathways and significantly reducing intracellular cholesterol levels. qPCR and western blot analyses confirmed the upregulation of key cholesterol synthesis regulatory factors such as SREBP2 and HMGCR, in response to tansospirone treatment. This metabolic perturbation, characterized by "cholesterol depletion-feedback activation", likely disrupts tumor cell lipid homeostasis, rendering cancer cells more vulnerable to cisplatin-induced apoptosis. Emerging evidence highlights the crucial role of cholesterol in tumor progression and therapy resistance^{24,25}. Cholesterol is not only a fundamental component of cell membranes but also regulates key signaling pathways, membrane microdomains, and apoptotic resistance mechanisms²⁶. Studies have suggested that lung cancer cells frequently upregulate cholesterol synthesis to evade chemotherapy-induced cell death^{27,28}. Cholesterol depletion may enhance apoptosis and chemosensitivity by disrupting lipid rafts, which are cholesterol-enriched membrane microdomains essential for pro-survival signaling. This disruption can impair pathways such as PI3K/AKT and MAPK/ERK, while altered membrane fluidity and receptor distribution may further sensitize tumor cells to chemotherapeutic agents. Our findings suggest that tansospirone, by depleting cholesterol and inducing metabolic stress, sensitizes tumor cells to chemotherapy. This effect was further corroborated by experiments showing that cholesterol depletion, whether induced by tansospirone or the cholesterol scavenger M β CD, enhanced the efficacy of multiple chemotherapeutic agents such as cisplatin, docetaxel, pemetrexed, bortezomib, and ML162. These results suggest that metabolic interventions targeting cholesterol depletion may serve as a broadly applicable chemosensitization strategy.

From a clinical perspective, this study holds dual significance. First, it provides critical safety evidence supporting the use of anti-ED medications in postoperative lung cancer patients, demonstrating that these drugs do not compromise chemotherapy efficacy. Second, our findings introduce a novel concept of "metabolic depletion-sensitization therapy," where an anxiolytic agent like tansospirone not only alleviates ED but also enhances chemotherapy effectiveness. This positions tansospirone as a promising candidate for integrated cancer care, particularly for patients experiencing both psychological distress and chemotherapy resistance.

This work has several limitations. This study found that chemotherapy is an independent risk factor for ED, but potential confounding factors may be associated with the results. Of note, other treatments can also increase

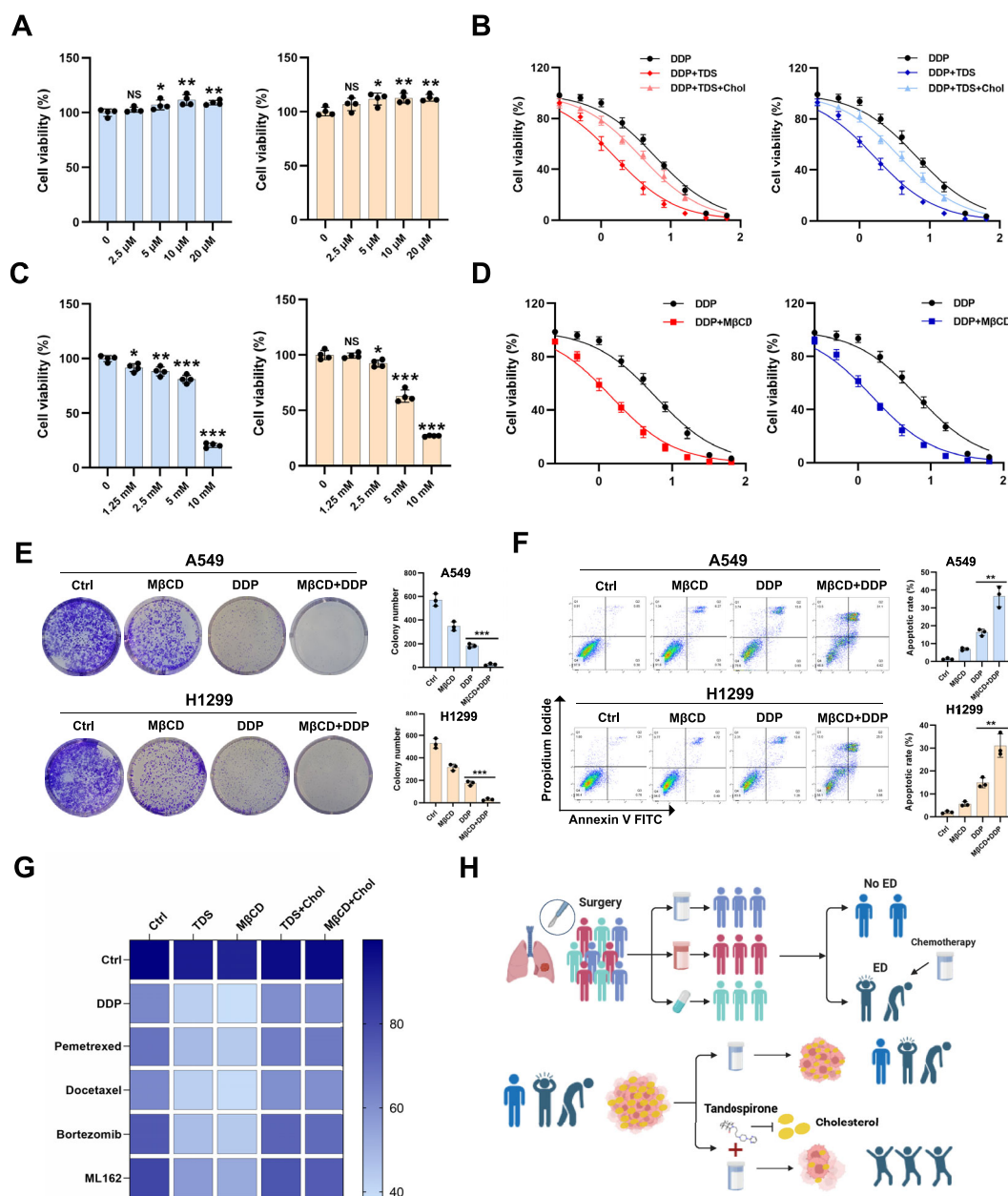


Fig. 6 | Lowering cholesterol levels in NSCLC cells can enhance their apoptosis sensitivity. **A** Cell viability values of A549 and H1299 cells after incubation with different concentrations of cholesterol for 48 h. **B** Cell viability values showed the effect of cholesterol (5 μ M) on the TDS effect of DDP. The x-axis values are expressed as $\log_{10}([DDP], \mu\text{M})$. **C** Cell viability values of A549 and H1299 cells after incubation with different concentrations of M β CD for 48 h. **D** Cell viability values show the effect of M β CD (2.5 mM) on the efficacy of DDP. The x-axis values are expressed as $\log_{10}([DDP], \mu\text{M})$. **E** A colony formation assay was performed to determine the effect of M β CD (2.5 mM) on the proliferation of DDP-treated A549 and H1299 cells. Quantitative analysis is presented on the right ($n = 3$). **F** Flow cytometry was performed to determine the effect of M β CD (2.5 mM) on apoptosis of

DDP-treated A549 and H1299 cells. Quantitative analysis is presented on the right ($n = 3$). **G** A heat map illustrating cell viability values (A549) showing the impact of cholesterol-depletion combined with various chemotherapeutic drugs and cell death-inducing agents, such as cisplatin, pemetrexed, docetaxel, bortezomib, and ML162. **H** The schematic diagram illustrates that chemotherapy increases the probability of ED in NSCLC patients and that tandospirone can enhance the efficacy of chemotherapy by regulating the cholesterol level (The figure was created with BioRender.com). Data are expressed as the mean \pm SD, $n = 3$, * $P < 0.05$, ** $P < 0.01$, *** $P < 0.001$.

patients' ED levels. Many studies have pointed out that ED affects the immune system, and it is unclear how anti-ED drugs affect immunotherapy in NSCLC patients. In addition, the machine learning-based risk prediction model developed in this study is only a preliminary proof-of-concept and was internally validated in a single center; multi-center external validation and further refinement are needed to improve its robustness and clinical applicability. Furthermore, as tandospirone is a clinically used anxiolytic, its safety profile when combined with chemotherapy warrants further

investigation. In the future, a larger sample size and corresponding clinical studies are warranted to further explore the safety and effectiveness of anti-ED drugs in combination with other treatments.

In conclusion, our study revealed that the ED status of postoperative lung cancer patients is closely related to adjuvant chemotherapy, and chemotherapy is an independent risk factor for ED. In addition to improving ED symptoms, common anti-ED drugs may improve lung cancer progression. Additional studies have found that tandospirone is safe and can

significantly improve the antitumor effect of cisplatin and promote cell apoptosis. Mechanistic exploration studies revealed that tandospirone reduces cholesterol levels in tumor cells, activates cholesterol synthesis-related genes such as SREBP2 and HMGCR, induces a “cholesterol depletion-death stress” state, and thus augments the killing effect of cisplatin. These findings offer a new scientific basis for the emotional management of postoperative lung cancer patients and lay a theoretical foundation for the rational use of anti-ED drugs in tumor treatment.

Methods

Study design and ethics statement

This single-center, cross-sectional study was approved by the Ethics Committee of the Shanghai Pulmonary Hospital affiliated with Tongji University (K22-184Y). The study protocol was in accordance with the relevant guidelines and regulations. This study followed the tenets of the Declaration of Helsinki. This study was anonymous, and the questionnaire used in the study did not collect any identifying information (e.g., name, hospital number), and the data were used only for statistical analyses. The Review Board and Ethics Committee of Shanghai Pulmonary Hospital (Shanghai, China) waived off the requirement for obtaining informed consent (ID: K22-184Y).

Study participants

This study involved 220 healthy volunteers and 1500 NSCLC patients who underwent surgery at the Shanghai Pulmonary Hospital between June 2022 and January 2024. The patient exclusion criteria included a history of neoadjuvant therapy, other malignancies within the past 3 years, psychiatric disorders, and any current antidepressant or anti-anxiety treatment. ED was assessed 6 month post-surgery. Ultimately, 192 volunteers and 1185 NSCLC patients were included in the final analyses.

Clinical characteristics

Patient data were collected and analyzed, including demographics (age, sex), medical history (hypertension, diabetes), lifestyle factors (smoking, drinking), education level, BMI, and postoperative medications (chemotherapy, targeted therapy, immunotherapy, etc.).

Evaluation of ED

ED generally refers to depression and/or anxiety symptoms. PHQ-9 and GAD-7 were used to screen these symptoms in cancer patients, with assessments conducted 6 months post-surgery^{29,30}. ED was defined as a PHQ-9 or GAD-7 score of ≥ 5 based on clinical thresholds⁵.

Data preprocessing and model building

Clinical and demographic characteristics of the patients, including age, gender, education level, and other relevant factors, were collected. The outcome variable was whether ED after surgery. The dataset was randomly divided into a training set and a test set in a 7:3 ratio. In the test set, model performance was evaluated using metrics such as the area under the receiver operating characteristic curve (AUC), accuracy, sensitivity, and specificity. To predict the risk of ED in postoperative lung cancer patients, this study employed two supervised machine learning algorithms: random forest (RF) and support vector machine (SVM). All analyses were performed in Python (version 3.9, Python Software Foundation), using scikit-learn for model construction and evaluation.

Cell culture

Human NSCLC cell lines (A549 and H1299) were obtained from Procell (Wuhan, China) and cultured in DMEM (BasalMedia, L110 KJ, China) supplemented with 10% FBS (Gibco, USA) and 1% penicillin/streptomycin (BasalMedia, S110JV) and incubated at 37 °C under a 5% CO₂ atmosphere.

Cell viability analysis

A549 and H1299 cells were seeded into 96-well plates and incubated under standard culture conditions. Anti-ED drugs (paroxetine, HY-

122272, MedChemExpress; sertraline, HY-B0176A, MedChemExpress; bupropion, HY-B0403, MedChemExpress; amitriptyline, HY-B0527, MedChemExpress; tandospirone, HY-14558, MedChemExpress; agomelatine, HY-17038, MedChemExpress), cholesterol (14606, Sigma-Aldrich) or methyl- β -cyclodextrin (M β CD, 332615, Sigma-Aldrich) or/and cisplatin, were added at varying concentrations based on the experimental protocol and cultured for 48 h. Next, fresh medium mixed with CCK-8 reagent (Beyotime, C0041) at a 10:1 ratio was added, and the cells were incubated at 37 °C for another 2 h. Absorbance was measured at 450 nm using a microplate reader (Infinite 200 PRO, Tecan). Cell viability was determined based on the average optical density (OD) values from at least three replicate wells.

Apoptosis analysis with flow cytometer

The experimental cells were plated into 12-well plates at a density of 3×10^5 cells/well and treated with anti-ED drugs, M β CD, and/or cisplatin. After 48 h of incubation, apoptosis was evaluated using an Annexin V-FITC/PI apoptosis detection kit (KeyGEN BioTECH, KGA1102) according to the manufacturer's protocol. Briefly, the cells were collected, washed thrice with PBS, and resuspended in 500 μ L of binding buffer. Then, 5 μ L of Annexin V-FITC and 5 μ L of PI were added, and the mixture was incubated in the dark at room temperature for 15 min. Flow cytometry data were obtained using the CytoFLEX S cytometer (Beckman, USA) and analyzed with FlowJo software (version 10).

Colony formation assay

Cells (500–1000/well) were seeded into six-well plates and incubated at 37 °C in a humidified atmosphere with 5% CO₂. Colonies were collected and washed with phosphate-buffered saline, fixed in 4% paraformaldehyde for 20 min, and stained with 0.5% crystal violet for 30 min. Images were captured using the Panoramic MIDI system.

Cell invasion, migration, and wound-healing assays

For the migration assay, A549 or H1299 (2×10^4) cells were seeded in a serum-free medium in the upper chamber (Corning Inc., Corning, NY, USA). For the invasion assay, the upper chamber was pre-coated with Matrigel (diluted 1:10; BD Biosciences, San Jose, CA, USA), and 5×10^5 cells were seeded in serum-free medium. The cells that migrated or invaded through the membrane were stained with 0.04% crystal violet and enumerated.

Animal models

BALB/c nude mice (4–6 weeks old) were obtained from Gempharmatech Co., Ltd. (Nanjing, China) and maintained under specific pathogen-free (SPF) conditions at Tongji University (Shanghai, China). No sex-based selection was applied in animal allocation. All animal procedures were conducted in accordance with the ARRIVE 2.0 guidelines and were approved by the Institutional Animal Care and Use Committee of the Shanghai Pulmonary Hospital affiliated with Tongji University. To assess in vivo tumor growth and metastatic potential, both subcutaneous xenograft and lung metastasis models were established. For the subcutaneous xenograft model, A549 cells (1×10^5 cells/injection) were inoculated into the left flank of mice. Drug treatments were initiated 2 weeks after tumor establishment. Tandospirone (20 mg/kg) and/or cisplatin (DDP, 2 mg/kg) were administered intraperitoneally every other day. Tumor size was measured weekly, and after 4 weeks, mice were euthanized by cervical dislocation, tumors were harvested for volumetric analyses. For the lung metastasis model, A549 cells (1×10^5 cells/dose) were injected via the tail vein, and the same drug administration regimen (tandospirone 20 mg/kg and/or DDP 2 mg/kg, intraperitoneally every other day) was applied. After 4 weeks, mice were euthanized by cervical dislocation, and lung metastases were analyzed by hematoxylin and eosin (H&E) staining.

Immunohistochemistry

Immunohistochemical (IHC) staining for Ki67 was conducted on paraffin-embedded tumor tissue sections in accordance with the experimental protocol. Images were captured using an inverted microscope (Olympus).

RNA sequencing

RNA high-throughput sequencing was performed using the Illumina HiSeq platform (Shanghai, China). Total RNA was first depleted of rRNA with the NEBNext rRNA Depletion Kit (New England Biolabs, Massachusetts, USA) following the manufacturer's instructions. RNA libraries were then constructed using the NEBNext® Ultra™ II Directional RNA Library Prep Kit (New England Biolabs) according to the provided protocol. Quality control and library quantification were assessed using the BioAnalyzer 2100 (Agilent Technologies, USA). Sequencing was conducted on the Illumina HiSeq system with 150 bp paired-end reads.

Isolation of lipid rafts

The experimental cells were seeded, treated with specified drugs, and harvested. They were then lysed in a buffer containing 20 mM Tris-HCl (pH 7.5), 150 mM NaCl, and 0.5% Triton X-100 for 30 min. The lysates were then centrifuged at 16,000 g at 4 °C for 30 min, and the supernatants were collected as non-lipid raft fractions. The remaining insoluble pellets were resuspended in 200 µL of buffer (0.5% SDS, 2 mM DTT) and incubated for 10 min. After another round of centrifugation under the same conditions, the supernatants were transferred into separate tubes as lipid raft fractions. The cholesterol levels were measured using the Amplex® Red Cholesterol Assay Kit (A12216, Invitrogen, Carlsbad, CA, USA)³¹.

Total RNA extraction and real-time quantitative polymerase chain reaction (RT-qPCR)

Total RNA was extracted using TRIzol reagent, and 2 µg of RNA was used for reverse transcription. RT-qPCR was conducted following the protocol provided in the UltraSYBR one-step RT-qPCR kit (CWBIO, Beijing, China). The primers used for the analysis are detailed in Supplementary Table 1.

Western blotting

Proteins from A549 and H1299 cells were extracted by using a total protein extraction kit. Protein concentrations were measured with a BCA protein assay kit. Proteins were separated via SDS-PAGE and transferred onto 0.45 µm polyvinylidene fluoride (PVDF) membranes (MilliporeSigma). The membranes were blocked with 5% non-fat dry milk for 1 h, then incubated overnight at 4 °C with primary antibodies targeting HMGCRCR (ab242315, Abcam), SREBP2 (ab30682, Abcam), and GAPDH (60004-1-Ig, Proteintech). The next day, membranes were incubated with the appropriate secondary antibody for 60 min at room temperature.

Statistical analysis

Continuous variables were expressed as the mean ± standard deviation. The χ^2 test was performed for the categorical comparison of demographic variables between different groups, whereas the Student's *t*-test and/or non-parametric test were applied for a continuous comparison. Skewness continuous variables were analyzed using median and interquartile range (IQR) and compared using the Mann-Whitney *U*-test. A logistic regression model was applied to evaluate factors affecting the occurrence of ED. The α -value < 0.05 on both sides was considered statistically significant. All statistical analyses were performed using SPSS 25.0 (SPSS, Inc., Chicago, IL, USA).

Data availability

No datasets were generated or analysed during the current study.

Code availability

The corresponding code for data preprocessing and model development is available from the corresponding author (xiedong@tongji.edu.cn) upon reasonable request for research purposes.

Received: 17 July 2025; Accepted: 23 September 2025;

Published online: 17 November 2025

References

- Leiter, A., Veluswamy, R. R. & Wisnivesky, J. P. The global burden of lung cancer: current status and future trends. *Nat. Rev. Clin. Oncol.* **20**, 624–639 (2023).
- Zhang, Y. T. et al. Global variations in lung cancer incidence by histological subtype in 2020: a population-based study. *Lancet Oncol.* **24**, 1206–1218 (2023).
- Hendriks, L. E. L. et al. Non-small-cell lung cancer. *Nat. Rev. Dis. Primers* **10**, 71 (2024).
- Li, J. et al. Effectiveness of mindfulness-based interventions on anxiety, depression, and fatigue in people with lung cancer: A systematic review and meta-analysis. *Int. J. Nurs. Stud.* **140**, 104447 (2023).
- Zeng, Y. et al. Association between pretreatment emotional distress and immune checkpoint inhibitor response in non-small-cell lung cancer. *Nat. Med.* **30**, 1680 (2024).
- Sullivan, D. R. et al. Depression symptom trends and health domains among lung cancer patients in the CanCORS study. *Lung Cancer* **100**, 102–109 (2016).
- Li, G. Z. et al. Effects of perioperative music therapy on patients with postoperative pain and anxiety: a systematic review and meta-analysis. *J. Integr. Complement* **30**, 37–46 (2024).
- Tola, Y. O., Chow, K. M. & Liang, W. Effects of non-pharmacological interventions on preoperative anxiety and postoperative pain in patients undergoing breast cancer surgery: a systematic review. *J. Clin. Nurs.* **30**, 3369–3384 (2021).
- Tian, L. X. et al. DNMT3a downregulation triggered upregulation of gaba receptor in the mpfc promotes paclitaxel-induced pain and anxiety in male mice. *Adv. Sci.* **12**, e2407387 (2025).
- Ning, L. et al. Hope and worry an interpretative phenomenological analysis of psychological experiences associated with targeted drug therapy among patients with advanced non-small-cell lung cancer. *Cancer Nurs.* **45**, E674–E679 (2022).
- Baralo, B. et al. Video education about side effects of chemotherapy and immunotherapy and its impact on the anxiety, depression, and distress level of cancer patients. *BMC Psychol.* **10**, 278 (2022).
- Duarte, D. & Vale, N. Antidepressant drug sertraline against human cancer cells. *Biomolecules* **12**, 1513 (2022).
- Radin, D. P. & Patel, P. A current perspective on the oncopreventive and oncolytic properties of selective serotonin reuptake inhibitors. *Biomed. Pharmacother.* **87**, 636–639 (2017).
- Abadi, B., Shahsavani, Y., Faramarzpour, M., Rezaei, N. & Rahimi, H. R. Antidepressants with anti-tumor potential in treating glioblastoma: a narrative review. *Fund. Clin. Pharm.* **36**, 35–48 (2022).
- Huang, X. F. et al. Role of tandospirone, a 5-HT_{1A} receptor partial agonist, in the treatment of central nervous system disorders and the underlying mechanisms. *Oncotarget* **8**, 102705–102720 (2017).
- Yamada, K., Yagi, G. & Kanba, S. Clinical efficacy of tandospirone augmentation in patients with major depressive disorder: a randomized controlled trial. *Psychiat Clin. Neuros* **57**, 183–187 (2003).
- Lu, X. Y. et al. Feeding induces cholesterol biosynthesis via the mTORC1-USP20-HMGCR axis. *Nature* **588**, 479 (2020).
- Trindade, B. C. et al. The cholesterol metabolite 25-hydroxycholesterol restrains the transcriptional regulator SREBP2 and limits intestinal IgA plasma cell differentiation. *Immunity* **54**, 2273 (2021).
- Guilbaud, E. et al. Cholesterol efflux pathways hinder KRAS-driven lung tumor progenitor cell expansion. *Cell Stem Cell* **30**, 800 (2023).
- Tan, C. R. C., Abdul-Majeed, S., Cael, B. & Barta, S. K. Clinical Pharmacokinetics and Pharmacodynamics of Bortezomib. *Clin. Pharmacokinet.* **58**, 157–168 (2019).
- Ma, F. R. et al. ML162 derivatives incorporating a naphthoquinone unit as ferroptosis/ apoptosis inducers: design, synthesis, anti-cancer

- activity, and drug-resistance reversal evaluation. *Eur. J. Med. Chem.* **270**, 116387 (2024).
22. Li, Y. T., Yan, B. S. & He, S. M. Advances and challenges in the treatment of lung cancer. *Biomed. Pharmacother* **169**, 115891 (2023).
 23. Ghoneim, M. M. & O'Hara, M. W. Depression and postoperative complications: an overview. *Bmc Surg.* **16**, 5 (2016).
 24. Huang, B. L., Song, B. L. & Xu, C. Q. Cholesterol metabolism in cancer: mechanisms and therapeutic opportunities. *Nat. Metab.* **2**, 132–141 (2020).
 25. Ding, X., Zhang, W. H., Li, S. & Yang, H. The role of cholesterol metabolism in cancer. *Am. J. Cancer Res.* **9**, 219–227 (2019).
 26. Luo, J., Yang, H. Y. & Song, B. L. Mechanisms and regulation of cholesterol homeostasis. *Nat. Rev. Mol. Cell Bio.* **21**, 225–245 (2020).
 27. Wu, Y. F. et al. Cholesterol reduces the sensitivity to platinum-based chemotherapy via upregulating ABCG2 in lung adenocarcinoma. *Biochem. Biophys. Res. Co.* **457**, 614–620 (2015).
 28. Daya, T., Breytenbach, A., Gu, L. & Kaur, M. Cholesterol metabolism in pancreatic cancer and associated therapeutic strategies. *Bba Mol. Cell Biol. L* **1870**, 159578 (2025).
 29. Deshields, T. L. et al. Addressing distress management challenges: recommendations from the consensus panel of the American psychosocial oncology society and the association of oncology social work. *Ca-Cancer J. Clin.* **71**, 407–436 (2021).
 30. Andersen, B. L., Rowland, J. H. & Somerfield, M. R. Screening, assessment, and care of anxiety and depressive symptoms in adults with cancer: an american society of clinical oncology guideline adaptation. *J. Oncol. Pr.* **11**, 133–U499 (2015).
 31. Pan, Z. Z. et al. Cholesterol promotes EGFR-TKIs resistance in NSCLC by inducing EGFR/Src/Erk/SP1 signaling-mediated ERR α re-expression. *Mol. Cancer* **21**, 77 (2022).

Acknowledgements

This research was supported by the National Key Research and Development Program of China (2024YFA1212000), the National Natural Science Foundation of China (82573733; 82372098; 82200999), the Shanghai Committee of Science and Technology China (21Y11913400), the Key Project of Jiangsu Provincial Health Commission (K2024044), the Open Projects of Jiangsu Provincial Key Laboratories (XZSYSKF2022012), the Key Project of Xuzhou Medical Science and Technology Innovation Project (XWKYHT20230034).

Author contributions

X.Q.: Investigation, Methodology, Data curation, Formal analysis, Writing—original draft. B.C.: Investigation, Methodology, Data curation, Formal analysis, Writing—original draft. S.M.: Methodology, Data curation, Formal

analysis. K.L.: Investigation, Methodology, Data curation, Writing—review and editing. Y.F.: Investigation, Data curation, Formal analysis. M.L.: Data curation, Formal analysis. R.W.: Methodology, Investigation. X.A.: Methodology, Investigation. L.W.: Investigation, Methodology, Data curation, Writing—review and editing. X.L.: Funding acquisition, Investigation, Writing—review and editing. X.W.: Funding acquisition, Conceptualization, Investigation, Supervision. D.X.: Funding acquisition, Investigation, Supervision, Writing—review and editing. All authors reviewed the manuscript.

Competing interests

The authors declare no competing interests.

Additional information

Supplementary information The online version contains supplementary material available at <https://doi.org/10.1038/s41746-025-02029-8>.

Correspondence and requests for materials should be addressed to Leilei Wu, Xiucheng Liu, Xiaojin Wu or Dong Xie.

Reprints and permissions information is available at <http://www.nature.com/reprints>

Publisher's note Springer Nature remains neutral with regard to jurisdictional claims in published maps and institutional affiliations.

Open Access This article is licensed under a Creative Commons Attribution-NonCommercial-NoDerivatives 4.0 International License, which permits any non-commercial use, sharing, distribution and reproduction in any medium or format, as long as you give appropriate credit to the original author(s) and the source, provide a link to the Creative Commons licence, and indicate if you modified the licensed material. You do not have permission under this licence to share adapted material derived from this article or parts of it. The images or other third party material in this article are included in the article's Creative Commons licence, unless indicated otherwise in a credit line to the material. If material is not included in the article's Creative Commons licence and your intended use is not permitted by statutory regulation or exceeds the permitted use, you will need to obtain permission directly from the copyright holder. To view a copy of this licence, visit <http://creativecommons.org/licenses/by-nc-nd/4.0/>.

© The Author(s) 2025